

Detecting and Receiving Phase-Modulated Signals With a Rydberg Atom-Based Receiver

Christopher L. Holloway^{ID}, *Fellow, IEEE*, Matthew T. Simons, *Member, IEEE*,
Joshua A. Gordon^{ID}, *Senior Member, IEEE*, and David Novotny

Abstract—The recent developments of Rydberg atom-based sensors with the ability to measure phase have made it possible to receive digital phase-modulated signals. In this letter, we demonstrate the reception of binary phase-shift keying, quadrature phase-shift keying, and quadrature amplitude modulation signals with an atom-based receiver. We present measured values of error vector magnitude as a function of symbol rate for various modulation schemes and discuss the bandwidth of a Rydberg atom-based receiver system. The results show that we can now interrogate ensembles of atoms to such extent that we can use them to receive data from a phase-modulated communication signal.

Index Terms—Atom-based receiver, atom-based sensor, binary phase-shift keying (BPSK), phase modulation, quadrature amplitude modulation (QAM), quadrature phase-shift keying (QPSK), Rydberg atoms.

I. INTRODUCTION

VARIOUS groups have begun investigating the use of Rydberg atom-based receivers for detecting and receiving communication signals, mainly due to the possible benefits and advantages they may have over conventional receiving systems. One of the widely used modulation schemes for transmitting data is phase modulation of a carrier wave. However, before we can evaluate the potential pros and cons of Rydberg atom communication receivers over conventional systems for receiving phase-modulated signals, we need to demonstrate that they can detect and receive data from this type of modulation scheme.

Rydberg atoms are atoms with one or more electrons excited to a very high principal quantum number n [1]. These Rydberg atoms have large dipole moments (scale as n^2), which make them very useful for electric (E) field sensors. The use of Rydberg states of an alkali atomic vapor placed in glass cells for radio frequency (RF) E -field strength and power sensors has made great strides in recent years [2]–[19]. Electromagnetically induced transparency (EIT) is used in this approach for E -field sensing, performed when an RF field is either on-resonance of a Rydberg transition [using Autler–Townes (AT) splitting] or off-resonance (using ac Stark shifts). This Rydberg atom-based sensor can act as a compact quantum-based receiver/antenna

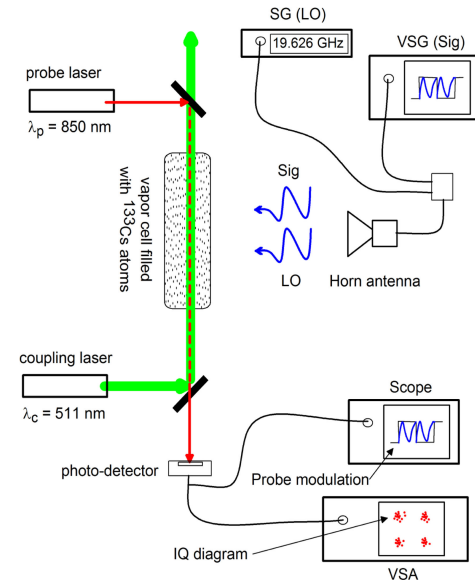


Fig. 1. Experimental setup for receiving digital phase-modulated signals.

for communication applications to detect and receive modulated signals.

The idea of a Rydberg receiver/antenna for modulated signals was demonstrated in [20]–[26]. Most of these demonstrations are limited to amplitude modulation (AM) and/or frequency modulation (FM) schemes. Digital AM was demonstrated in [20] and [26]. One form of phase modulation was shown in [20], where the phase of the AM was detected as a digital signal. However, in order to detect and receive carrier phase-modulated signals [the basis of most digital modulation schemes, e.g., binary phase-shift keying (BPSK), quadrature phase-shift keying (QPSK), and quadrature amplitude modulation (QAM)], detection of the phase of the carrier RF signal is required. This EIT scheme has been very successful in detecting the amplitude of continuous-wave (CW) carriers. However, the ability to measure the phase of an RF signal with Rydberg atom-based receivers has not been possible until recently [27].

The motivation of this letter is to investigate the use of the quantum-based E -field sensor technology in the area of communications for phase-modulation reception. To this end, we use the Rydberg atom-based mixer (depicted in Fig. 1), which was recently developed [27], [28], to demonstrate the ability to detect a phase-modulated RF carrier and, in turn, detect and

Manuscript received July 2, 2019; accepted July 22, 2019. Date of publication July 29, 2019; date of current version September 4, 2019. (Corresponding author: Christopher L. Holloway.)

The authors are with the National Institute of Standards and Technology, Boulder, CO 80305 USA (e-mail: christopher.holloway@nist.gov; matthew.simons@nist.gov; josh.gordon@nist.gov; david.novotny@nist.gov).

Digital Object Identifier 10.1109/LAWP.2019.2931450

receive BPSK, QPSK, and QAM signals. We emphasize that just because one can measure the phase of the CW field (as was done in [27]) does not mean one can detect and receive data for a phase-modulated communication signal. Therefore, we show how the Rydberg atom-based technique along with the atom-based mixer can detect and receive data from different phase-modulation schemes that are used in typical communication systems.

II. MEASURING PHASE OF A SIGNAL AND RECEIVING SYMBOLS IN A COMMUNICATION SIGNAL

A widely used modulation scheme for digital communications is phase-shift keying (PSK) using both BPSK and QPSK [29]. In these modulation schemes, data are transmitted by changing (or modulating) the phase of the CW carrier. BPSK uses two different phase states to transmit data, in which the carrier frequency phase is changed between 0° and 180° . Each phase state represents one transmitted symbol, and each symbol is mapped into bits “1” or “0.” QPSK is a type of PSK, where each transmitted symbol (or phase state) is mapped into two bits. This is done by choosing one of four possible phases applied to a CW carrier [e.g., 45° (binary state “00”), 135° (binary state “01”), -45° (binary state “10”), and -135° (binary state “11”)]. Using both the phase and the amplitude, this idea is extended to QAM, where 16QAM corresponds to 16 phase and amplitude states; each phase state is a transmitted symbol (each symbol corresponds to 4 bits, “0000,” “1000,” “1100,” etc.). Continuing this, (2^n) QAM corresponds to 2^n phase and amplitude states; each phase state is a transmitted symbol (each symbol corresponds to n bits). Thus, to receive BPSK, QPSK, and QAM signals, one needs to measure and detect the phase and amplitude of the CW carrier. The Rydberg atom-based mixer [27] allows us to measure the phase and amplitude of a carrier, and we use this approach to receive BPSK, QPSK, 16QAM, 32QAM, and 64QAM modulated signals.

Details of how the atom-based mixer works are given in [27], and we give a brief discussion here. A reference RF field (labeled “LO” in Fig. 1) on-resonance with the Rydberg atom transition acts as a local oscillator (LO). The “LO” field causes the EIT/AT effect in the Rydberg atoms, which is used to downconvert a second copolarized RF field. This second field is detuned from the “LO” field and is the digital modulated carrier (labeled “SIG” in Fig. 1). The frequency difference between the LO and the SIG is an intermediate frequency (IF), and the IF is detected by optically probing the Rydberg atoms (see Fig. 1). The phase of the IF signal corresponds directly to the relative phase between the “LO” and “SIG” signals. In effect, the atom-based mixer does all the downconversion of the “SIG” and the “LO,” and a direct read-out of the phase of SIG is obtained by the probe laser propagating through the atomic vapor. By measuring the relative phase shift of the IF signal (via a photodetector), we can determine the phase states of BPSK, QPSK, and QAM signals.

The EIT/AT technique involves monitoring the transmission of a “probe” laser through the vapor cell. A second laser (“coupling” laser) establishes a coherence in the atomic states and enhances the probe transmission through the atoms. An applied RF field (the LO field in our case) alters the susceptibility

of the atomic vapor, which results in a change in the probe laser transmission. As shown in [27], the presence of both LO and SIG fields creates a beat note, and the beat note results in AM of the probe transmission, where the amplitude of the probe transmission varies as $\cos(2\pi f_{\text{IF}} t + \Delta\phi)$ (where f_{IF} is the frequency of the IF field and $\Delta\phi$ is the phase difference between the LO and SIG fields). This AM of the probe laser transmission can be detected with a photodetector and used to determine the phase of the SIG signal. For a pure AM or FM carrier, the Rydberg atoms automatically demodulate the carrier, and output of the photodetector gives a direct read-out of the baseband signal (the information being transmitted). For a phase-modulated carrier, the Rydberg atoms automatically downconvert the carrier to the IF, which contains the phase states of the different phase-modulation schemes.

III. EXPERIMENTAL RESULTS

A diagram of the experimental setup is shown in Fig. 1. To generate EIT, we use cesium (^{133}Cs) atoms. The probe laser is tuned to the D_2 transition for ^{133}Cs ($6S_{1/2}-6P_{3/2}$ or wavelength of $\lambda_p = 850.53$ nm) focused to a full-width at half-maximum (FWHM) of $425\ \mu\text{m}$, with a power of $41.2\ \mu\text{W}$. To produce an EIT signal, we couple to the ^{133}Cs $6P_{3/2}-34D_{5/2}$ states by applying a counterpropagating coupling laser at $\lambda_c = 511.1480$ nm with a power of $48.7\ \text{mW}$, focused to an FWHM of $620\ \mu\text{m}$. We use a signal generator (SG) to apply an LO field at $19.626\ \text{GHz}$ to couple states $34D_{5/2}$ and $35P_{3/2}$. While we use $19.626\ \text{GHz}$ in these experiments, this approach can work at carriers from $100\ \text{MHz}$ to $1\ \text{THz}$ (because of the broadband nature of the EIT/AT approach [2], [3]). To generate the modulated SIG field, we use a vector signal generator (VSG). The VSG applies a given digital modulation scheme AM and/or phase to a CW carrier. We set the frequency of the CW SIG field to $19.626\ \text{GHz}+f_{\text{IF}}$ (where the f_{IF} is changed during these experiments). The outputs from the SG and the VSG were connected to a standard gain horn antenna via a power combiner. The output of the photodetector was connected to the input of a vector signal analyzer (VSA). The Rydberg atoms automatically downconvert the modulated carrier to the IF (the amplitude of the probe laser transmission), and the signal analyzer can detect the phase change of the IF signal and, hence, detect the phase state of the signal. In effect, the VSA detects the phase state of a downconverted signal and, hence, recovers the phase state of the modulated carrier. The output of the photodetector was also sent to an oscilloscope.

We first demonstrate the ability to receive a BPSK signal. Fig. 2 shows the signal detected on the photodetector (measured on the oscilloscope) for a BPSK modulation for $f_{\text{IF}} = 500\ \text{kHz}$ and symbol period of $1\ \mu\text{s}$ (i.e., a symbol rate of $1\ \text{kSym/s}$ or $1\ \text{kb/s}$). Also, in the figure, there is a reference signal. Comparing the reference signal with the photodetector signal shows the phase shift in the signal when the symbol state changes (represented by the square wave in the figure). Furthermore, comparing the phase of the beat-note (or photodetector) signal to the reference signal in each symbol frame gives the phase of the CW carrier in that symbol, i.e., the phase state of the CW in the particular symbol.

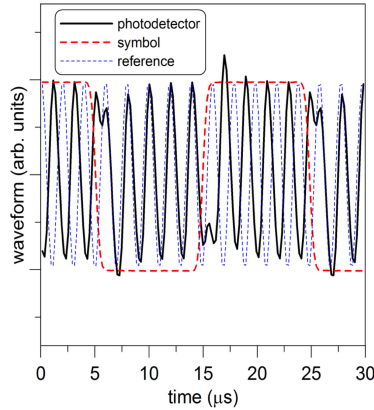


Fig. 2. Signal detected on the photodetector (measured on the oscilloscope) for BPSK modulation for $f_{IF} = 500$ kHz and symbol rate of 100 kSym/s (symbol period of 10 μ s).

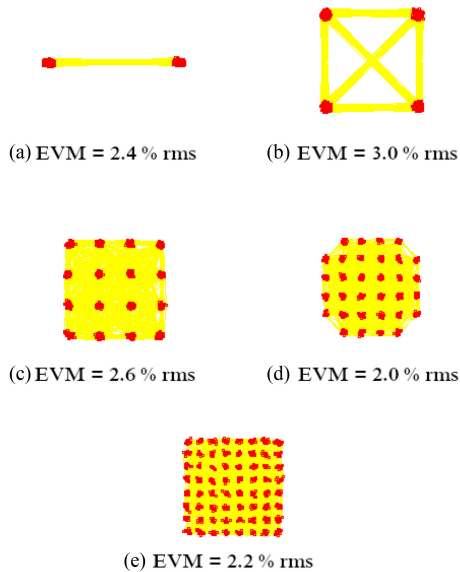


Fig. 3. Measured IQ diagrams: (a) BPSK, (b) QPSK, (c) 16QAM, (d) 32QAM, and (e) 64QAM. The EVM for each case is indicated as well. The bandwidth of both the photodetector and the VSA is 10 MHz.

In communications, an IQ constellation diagram (IQ stands for in-phase and quadrature components of the modulated signal; also called a polar or vector diagram) is typically used to represent the phase state of a symbol (i.e., in our case the phase and amplitude of the IF signal). Furthermore, a metric to assess how well a digital signal (a bit stream) is detected is the error vector magnitude (EVM) [30]. EVM is an error vector of the measured (received) phase/amplitude state compared to the ideal state and is basically an assessment of the received modulation quality. The VSA can generate the IQ diagram for the detected signal and calculate the EVM of the received bit stream. The IQ diagram for receiving 2047 symbols is shown in Fig. 3. Fig. 3 shows the received IQ diagrams for the Rydberg atom receiver for five different modulation schemes (BPSK, QPSK, 16QAM, 32QAM, and 64QAM), each with an IF = 1 MHz and the symbol rate of 100 kSym/s. The grouping of the data is that various quadrants correspond to the reception of the possible phase/amplitude states for the different modulation schemes.

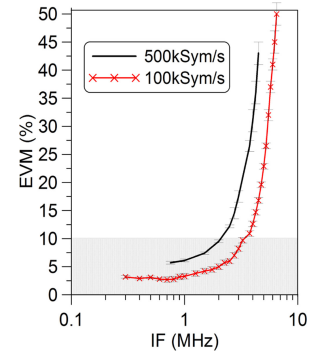


Fig. 4. Measured EVM for BPSK for different IF. The error bars represent the variability in the measured EVM. The bandwidth of both the photodetector and the VSA is 10 MHz.

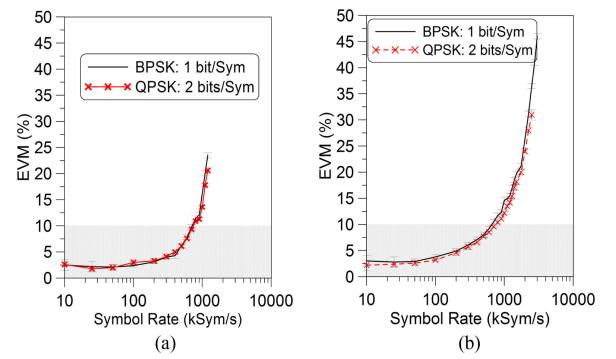


Fig. 5. Measured EVM for BPSK and QPSK. (a) IF = 1 MHz and (b) IF = 2 MHz. The bandwidth of both the photodetector and the VSA is 10 MHz.

We first looked at the bandwidth of the Rydberg atom-based receiver. This bandwidth limit is due to the time required to populate the atoms to a Rydberg state. A numerical time-domain calculation of the master equation for the density matrix components given in [14] shows that the population of the Rydberg state reaches steady state around 1 μ s, but has significant population by 0.1–0.3 μ s, which implies that the atoms can respond on the order of 3–10 MHz. As we will see, while the Rydberg state may not be fully populated in 0.3 μ s (3 MHz), the atom-based mixer can detect and receive digital signals for data rate above 5 MHz (but the EVM starts to become large). For this atom-based mixer approach, varying the IF value gives an indication of the maximum data rate for digital signals that can be detected. In effect, the atoms respond to the IF signal; as a result, the higher the IF, the faster the atoms have to respond. Fig. 4 shows the EVM as a function of IF for a BPSK signal for two different symbol rates. We see that at around 1 MHz, the EVM starts to increase, and at around 2–3 MHz, the EVM increases above 10%, but data are still received for IF > 3 MHz. Next, we set IF to 1 and 2 MHz, then varied the symbol rate. Fig. 5 shows the EVM as a function of symbol rate for BPSK. Here, we see that the EVM is below 5% for symbol rates below 400 kSym/s for both IF values. The EVM approaches 10% for symbol rate around 700 kSym/s in both cases. The EVM continues to increase with increasing symbol rate. We should point out that, as one might expect, once the period of the IF becomes smaller than the symbol period, it becomes difficult to detect the different phases of the carrier

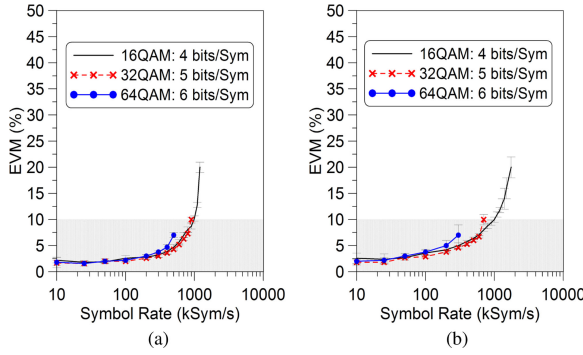


Fig. 6. Measured EVM for 16QAM, 32QAM, and 64QAM. (a) IF = 1 MHz and (b) IF = 2 MHz. The bandwidth of both the photodetector and the VSA is 10 MHz.

(i.e., when the IF wavelength is larger than the symbol length). While the high symbol rates are approaching the bandwidth of the Rydberg atoms, the atom-based mixer still detects and receives BPSK signals with the caveat that the EVM does increase with high symbol rate.

Next, we transmitted a QPSK signal (an example of an IQ diagram is shown in Fig. 3). The EVM for QPSK versus symbol rate is shown in Fig. 5. We see that the QPSK follows the BPSK results. However, keep in mind that the QPSK transmits 2 bits/symbol, while BPSK transmits only 1 bit/symbol. Here, again, once the period of the IF becomes smaller than the symbol rate, it becomes difficult to detect the phase states of the carrier.

Finally, we transmitted 16QAM, 32QAM, and 64QAM signals (IQ diagrams are shown in Fig. 3). These 16QAM, 32QAM, and 64QAM are actually transmitting 4 bits/symbol, 5 bits/symbol, and 6 bits/symbol, respectively. The EVMs for 16QAM, 32QAM, and 64QAM are shown in Fig. 6. From the IQ diagrams, we see that the phase states for the various QAM schemes become more crowded as the number of bits per symbol increases (i.e., going from 16QAM to 32QAM). As such, a small error in the phase states will affect 64QAM more than 16QAM. This is indicated in the EVM data shown in Fig. 6. The point where 32QAM cannot be received (the right side of the EVM curve where the data stop) occurs at a smaller symbol rate than the point where 16QAM cannot be received, and 64QAM falls off even faster.

While BPSK and QPSK are pure phase-modulation schemes, QAM requires modulation of both the phase and the amplitude. The detected amplitudes from the atom-based mixer drops with higher IF values [27], and it becomes hard to distinguish changes in the amplitude (required for the QAM scheme). This explains why the QAM scheme degrades before BPSK and QPSK schemes.

IV. CONCLUSION AND DISCUSSION

The results in this letter illustrate the capability of using a Rydberg atom-based mixer to detect and receive various phase and amplitude digital modulation schemes (BPSK, QPSK, 16QAM, 32QAM, and 64QAM). The atom-based mixer can detect and receive digital signals as the transmitted symbol rate approaches the bandwidth of the Rydberg atom response, which is around 1–10 MHz (and is likely the limit of the IF that can be used

for the Rydberg atom-based mixer). The EVM does increase with symbol rate, though data can be received even for high EVM through the use of error correction techniques. While the advantages of a Rydberg atom-based digital receiver have not been fully explored, the atom-based mixer potentially has many benefits over conventional technologies in detecting and receiving modulated signals. For example:

- 1) no need for traditional demodulation/downconversion electronics because the atoms automatically perform the demodulation for AM and FM signals [20], [22], [25], [26] and automatically downconvert the phase-modulated signals to an IF;
- 2) micrometer-sized antennas and receivers over a frequency range of 100 MHz to 1 THz [2], [3];
- 3) no Chu limit [31] requirements as is the case for standard antennas;
- 4) direct real-time read-out;
- 5) multiband (or multichannel) operation in one compact vapor cell [22], [23];
- 6) the possibility of electromagnetic interference-free receiving;
- 7) ultrahigh sensitivity reception from 100 MHz to 1 THz [28].

In fact, in [28], it is shown that field levels down to $40 \mu\text{V/m}$ are detectable, and using a field enhancement technique such as that shown in [32], much lower field levels are possible. Furthermore, there are indications that this Rydberg atom-based system may be less susceptible to noise. As was the case in measuring CW electric-field strengths [19], where we performed experiments measuring CW *E*-field strengths using this atom-based approach in the presence of band-limited white Gaussian noise, we showed that the *E*-field strength could be detected in low CW-signal-to-noise-power ratio conditions. Other noise studies are shown in [22]. The detection scheme discussed here can be improved by reducing laser noise and systematic effects, which is the topic of future work.

The field of Rydberg atom-based sensors is in its infancy, and for these systems to be economically feasible, several technologies will need to be improved and developed. For example, compact and inexpensive coupling lasers are needed. There are a few groups currently investigating the commercialization of such lasers. While other developments are required to mature this technology, the potential advantage of the atom-based systems has accelerated the interest of many groups (including universities, private companies, and government agencies) to investigate a wide array of possible applications, including the use as communication receivers as we have demonstrated.

While more research is needed to fully understand the advantages of the Rydberg atom approach over conventional radio technologies, the study reported here illustrates the capability of a Rydberg atom-based receiver/antenna system to detect and demodulate BPSK, QPSK, and QAM signals. In effect, we are now in a position to be able to interrogate ensembles of atoms to such accuracy that we can use them to receive data from phase-modulation schemes widely used today for digital communications.

REFERENCES

- [1] T. F. Gallagher, *Rydberg Atoms*. Cambridge, U.K.: Cambridge Univ. Press, 1994.
- [2] C. L. Holloway *et al.*, “Atom-based RF electric field metrology: From self-calibrated measurements to sub-wavelength and near-field imaging,” *IEEE Trans. Electromagn. Compat.*, vol. 59, no. 2, pp. 717–728, Apr. 2017.
- [3] C. L. Holloway *et al.*, “Broadband Rydberg atom-based electric-field probe for SI-traceable, self-calibrated measurements,” *IEEE Trans. Antennas Propag.*, vol. 62, no. 12, pp. 6169–6182, Dec. 2014.
- [4] J. A. Sedlacek, A. Schwettmann, H. Kubler, R. Low, T. Pfau, and J. P. Shaffer, “Microwave electrometry with Rydberg atoms in a vapour cell using bright atomic resonances,” *Nature Phys.*, vol. 8, pp. 819–824, 2012.
- [5] C. L. Holloway *et al.*, “Sub-wavelength imaging and field mapping via electromagnetically induced transparency and Autler–Townes splitting in Rydberg atoms,” *Appl. Phys. Lett.*, vol. 104, 2014, Art. no. 244102.
- [6] J. A. Sedlacek, A. Schwettmann, H. Kubler, and J. P. Shaffer, “Atom-based vector microwave electrometry using rubidium Rydberg atoms in a vapor cell,” *Phys. Rev. Lett.*, vol. 111, 2013, Art. no. 063001.
- [7] J. A. Gordon *et al.*, “Millimeter wave detection via Autler–Townes splitting in rubidium Rydberg atoms,” *Appl. Phys. Lett.*, vol. 105, 2014, Art. no. 024104.
- [8] H. Fan, S. Kumar, J. Sedlacek, H. Kubler, S. Karimkashi, and J. P. Shaffer, “Atom based RF electric field sensing,” *J. Phys. B: Atom. Mol. Opt. Phys.*, vol. 48, 2015, Art. no. 202001.
- [9] M. Tanasitikosol *et al.*, “Microwave dressing of Rydberg dark states,” *J. Phys. B*, vol. 44, 2011, Art. no. 184020.
- [10] C. G. Wade, N. Sibalic, N. R. de Melo, J. M. Kondo, C. S. Adams, and K. J. Weatherill, “Real-time near-field terahertz imaging with atomic optical fluorescence,” *Nature Photon.*, vol. 11, pp. 40–43, 2017.
- [11] D. A. Anderson, S. A. Miller, G. Raithel, J. A. Gordon, M. L. Butler, and C. L. Holloway, “Optical measurements of strong microwave fields with Rydberg atoms in a vapor cell,” *Phys. Rev. Appl.*, vol. 5, 2016, Art. no. 034003.
- [12] D. A. Anderson *et al.*, ‘Two-photon microwave transitions and strong-field effects in a room-temperature Rydberg-atom gas,’ *Phys. Rev. A*, vol. 90, 2014, Art. no. 043419.
- [13] A. K. Mohapatra, T. R. Jackson, and C. S. Adams, “Coherent optical detection of highly excited Rydberg states using electromagnetically induced transparency,” *Phys. Rev. Lett.*, vol. 98, 2007, Art. no. 113003.
- [14] C. L. Holloway, M. T. Simons, J. A. Gordon, A. Dienstfrey, D. A. Anderson, and G. Raithel, “Electric field metrology for SI traceability: Systematic measurement uncertainties in electromagnetically induced transparency in atomic vapor,” *J. Appl. Phys.*, vol. 121, 2017, Art. no. 233106.
- [15] M. T. Simons, J. A. Gordon, and C. L. Holloway, “Using frequency detuning to improve the sensitivity of electric field measurements via electromagnetically induced transparency and Autler–Townes splitting in Rydberg atoms,” *Appl. Phys. Lett.*, vol. 108, 2016, Art. no. 174101.
- [16] M. T. Simons, J. A. Gordon, and C. L. Holloway, “Simultaneous use of Cs and Rb Rydberg atoms for dipole moment assessment and RF electric field measurements via electromagnetically induced transparency,” *J. Appl. Phys.*, vol. 102, 2016, Art. no. 123103.
- [17] C. L. Holloway, M. T. Simons, M. D. Kautz, A. H. Haddab, J. A. Gordon, and T. P. Crowley, “A quantum-based power standard: Using Rydberg atoms for a SI-traceable radio-frequency power measurement technique in rectangular waveguides,” *Appl. Phys. Lett.*, vol. 113, 2018, Art. no. 094101.
- [18] M. T. Simons, J. A. Gordon, and C. L. Holloway, “Fiber-coupled vapor cell for a portable Rydberg atom-based radio frequency electric field sensor,” *Appl. Opt.*, vol. 57, no. 22, pp. 6456–6460, 2018.
- [19] M. T. Simons, M. D. Kautz, C. L. Holloway, D. A. Anderson, and G. Raithel, “Electromagnetically induced transparency (EIT) and Autler–Townes (AT) splitting in the presence of band-limited white Gaussian noise,” *J. Appl. Phys.*, vol. 123, 2018, Art. no. 203105.
- [20] D. H. Meyer, K. C. Cox, F. K. Fatemi, and P. D. Kunz, “Digital communication with Rydberg atoms and amplitude-modulated microwave fields,” *Appl. Phys. Lett.*, vol. 12, 2018, Art. no. 211108.
- [21] K. C. Cox, D. H. Meyer, F. K. Fatemi, and P. D. Kunz, “Quantum-limited atomic receiver in the electrically small regime,” *Phys. Rev. Lett.*, vol. 121, 2018, Art. no. 110502.
- [22] C. L. Holloway *et al.*, “A multiple-band Rydberg-atom based receiver/antenna: AM/FM stereo reception,” *IEEE Antennas Propag. Mag.*, submitted for publication.
- [23] D. A. Anderson, R. E. Sapiro, and G. Raithel, “An atomic receiver for AM and FM radio communication,” 2018, *arXiv:1808.08589v1*.
- [24] C. L. Holloway, M. T. Simons, A. H. Haddab, C. J. Williams, and M. W. Holloway, “A real-time guitar recording using Rydberg atoms and electromagnetically induced transparency: Quantum physics meets music,” *AIP Adv.*, vol. 9, no. 6, 2019, Art. no. 065110.
- [25] A. B. Deb and N. Kjaergaard, “Radio-over-fiber using an optical antenna based on Rydberg states of atoms,” *Appl. Phys. Lett.*, vol. 112, 2018, Art. no. 211106.
- [26] Z. Song *et al.*, “The credibility of Rydberg atom based digital communication over a continuously tunable radio-frequency carrier,” *Opt. Express*, vol. 27, no. 6, pp. 8848–8857, 2019.
- [27] M. T. Simons, A. H. Haddab, J. A. Gordon, and C. L. Holloway, “A Rydberg atom-based mixer: Measuring the phase of a radio frequency wave,” *Appl. Phys. Lett.*, vol. 114, 2019, Art. no. 114101.
- [28] J. A. Gordon, M. T. Simons, and C. L. Holloway, “Weak electric-field detection with sub-1 Hz resolution at radio frequencies using a Rydberg atom-based mixer,” *AIP Adv.*, vol. 9, 2019, Art. no. 045030.
- [29] T. S. Rappaport, *Wireless Communications: Principles and Practice*. Upper Saddle River, NJ, USA: Prentice-Hall, 1996, ch. 5.
- [30] M. D. McKinley, K. A. Remley, M. Myslinski, J. S. Kenney, D. Schreurs, and B. Nauwelaers, “EVM calculation for broadband modulated signals,” in *64th Autom. Radio Freq. Techn. Group Conf. Dig.*, 2004, pp. 45–62.
- [31] L. J. Chu, “Physical limitations of omnidirectional antennas,” *J. Appl. Phys.*, vol. 19, 1948, Art. no. 1163.
- [32] D. A. Anderson, E. G. Paradis, and G. Raithel, “A vapor-cell atomic sensor for radio-frequency field detection using a polarization-selective field enhancement resonator,” *Appl. Phys. Lett.*, vol. 113, 2018, Art. no. 073501.